

Spin-Wave Nonlinear Dynamics in an Yttrium Iron Garnet Sphere

Paul Bryant^(a) and Carson Jeffries

*Physics Department, University of California, Berkeley, California 94720, and
Materials and Chemical Sciences Division, Lawrence Berkeley Laboratory, Berkeley, California 94720*

and

Katsuhiko Nakamura

Fukuoka Institute of Technology, Higashi-ku, Fukuoka 811-02, Japan

(Received 26 January 1988)

A high-resolution experiment is reported for spin-wave dynamics in an yttrium iron garnet sphere. For certain parameter values we observe a series of closely spaced spin-wave modes. Interactions between excited modes lead to various dynamical phenomena including auto-oscillations, period-doubling cascades, quasiperiodicity, and chaos. Also observed are irregular relaxation oscillations, abrupt transitions to wide-band turbulence, and hysteresis at the Suhl threshold. A theoretical model is studied analytically and numerically, explaining a number of the experimental behavior patterns.

PACS numbers: 76.50.+g, 05.45.+b, 47.20.Tg, 75.30.Ds

Spin-wave instabilities were first observed^{1,2} as noisy anomalous absorption when microwave ferromagnetic absorption was strongly driven; Suhl³ gave a theory of this behavior and remarked (1957), “. . . this situation bears a certain resemblance to the turbulent state in fluid dynamics . . .,” a viewpoint recently validated by studies of spin-wave dynamics within the framework of nonlinear dynamics, which views spin waves in a ferromagnetic sphere as a set of coupled modes, with the dynamics controlled by a low-dimensional attractor. It was predicted⁴ and observed⁵ that excited spin waves may show a period-doubling route to chaos; further theoretical⁶⁻¹⁰ and experimental¹¹⁻¹⁴ studies followed. We report here a high-resolution (10^{-5}) study of the first-order perpendicular pumped instability (“subsidiary absorption”) in an yttrium iron garnet sphere, finding strikingly rich behavior in different regions of parameter space, including single-mode excitation; low-frequency collective oscillations when two modes are excited; quasiperiodicity, locking, and chaos when three modes are excited; and abrupt hysteretic onset of wide-band chaos at the Suhl threshold. We show that much of this behavior can be understood from stability analysis and numerical iteration of a new theoretical model of coupled modes.

In the experiment, spins on the ferrite lattice subject to fields \mathbf{H}_0 and $\mathbf{H}_1 \sin \omega_p t$ display a narrow ferromagnetic resonance when $\gamma H_0 = \omega_p$, with $\gamma = 1.77 \times 10^7 \text{ s}^{-1}$ and $\omega_p = 5.79 \times 10^{10} \text{ s}^{-1}$. In addition to this uniform precession mode, the Heisenberg exchange gives rise to spin waves.¹⁵ A spin-wave pair, (ω_k, k) and $(\omega_k, -k)$, i.e., a “mode,” is excited at half field for $\gamma H_0 = (\omega_p/2) = \omega_k$ if H_1 exceeds the Suhl threshold for the first mode to go unstable. The experiment is performed at $T = 300 \text{ K}$ with a sphere of pure single-crystal yttrium iron garnet (diameter $d = 0.066 \text{ cm}$, spherical to 6×10^{-5} , smooth to $0.15 \text{ } \mu\text{m}$) mounted in a resonator with the crystal axis

$[111] \parallel \mathbf{H}_0 \perp \mathbf{H}_1$ and incident microwave power $P_i \propto H_1^2$ from a klystron oscillator coupled via wave guide and precision attenuator. Power not absorbed is reflected to a detector, yielding a dc signal S_0 and also a low-frequency signal $S(t)$. Figure 1 shows regions and boundaries of types of observed behavior in the parameter space (P_i, H_0) . As P_i and H_0 are varied, the Suhl threshold is marked by a decrease in S_0 which is abrupt (within 0.05 dB) and reversible except in the shaded area ($1200 < H_0 < 1600 \text{ G}$) where it is abrupt and hysteretic, and accompanied by a large increase (50 dB) in $S(t)$ of wide-band character, with no resolvable spectral peaks. In the region $H \gtrsim 1600 \text{ G}$ and $P_i \approx 0.1 \text{ dB}$ above the Suhl threshold, we observe collective oscillations (“auto-oscillations”) at 10^4 to 10^6 Hz , arising from the coupling between microwave spin-wave modes (10^{10} Hz). Their origin is revealed by a high-resolution exam-

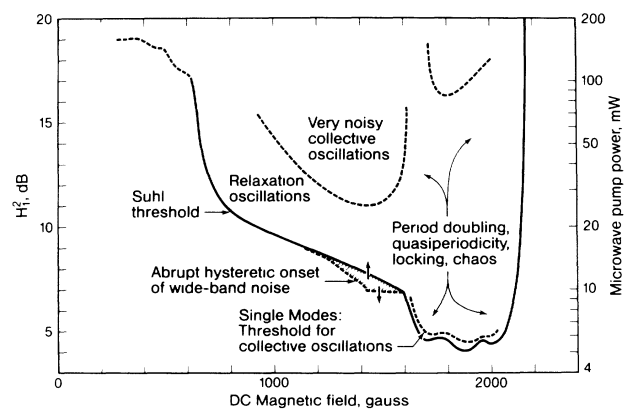


FIG. 1. Regions and boundaries of types of experimentally observed behavior in the perpendicular-pumped spin-wave instability in an yttrium iron garnet sphere; dc field H_0 vs microwave pump power $P_i \propto H_1^2$.

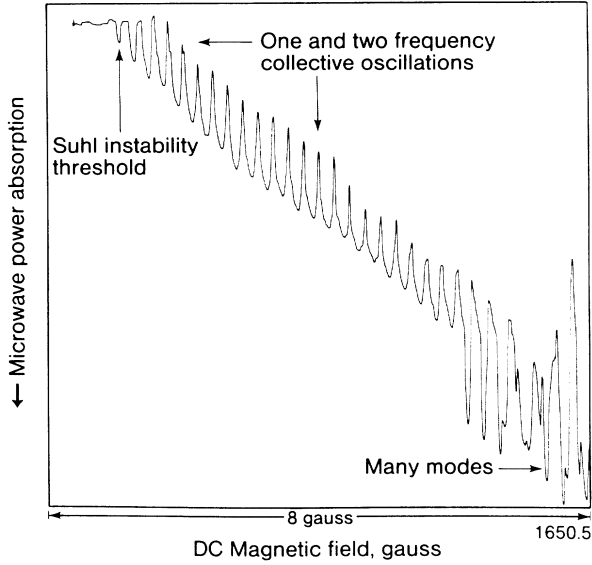


FIG. 2. Microwave absorption in an yttrium iron garnet sphere as the magnetic field is increased through the Suhl threshold, showing sequence of single spatial spin-wave modes, spaced by $\Delta H_0 \approx 0.157$ G.

ination of the Suhl threshold, showing a series of peaks (Fig. 2) separated by $\Delta H_0 = 0.157$ G; these can be understood as high-order spatial resonances of single spin-wave modes within the sphere, as originally noted by Jantz and Schneider.¹⁶ For a small change, $\Delta k = \pi/d$, the field change computed from the dispersion relation is 0.152 G for $k = 3 \times 10^5 \text{ cm}^{-1}$. The first few dips in S_0 are not accompanied by an ac signal, an indication that only a single microwave mode is excited at each dip. As H_0 is increased, simultaneous excitation of two modes is possible, and a sinusoidal signal may arise [Fig. 3(a)], corresponding to a Hopf bifurcation. This collective oscillation shows period doubling [Fig. 3(b)] and sometimes a cascade to chaos [Fig. 3(e)]. The frequency f_{c0} depends partially on the dynamic interaction of the two modes and hence on P_i ; the data are fitted by the expression $f_{c0}^2 = K[(P_i/P_{ic}) - 1]$, where P_{ic} is the oscillation threshold pump power; this dependence is predicted by our model and is also suggested by the work of Zautkin, L'vov, and Starobinets.¹⁷

These oscillations do not usually complete a cascade to chaos before interruption by the appearance of a second, incommensurate frequency f'_{c0} , [Fig. 3(c)] associated with the excitation of a third microwave mode. The sys-

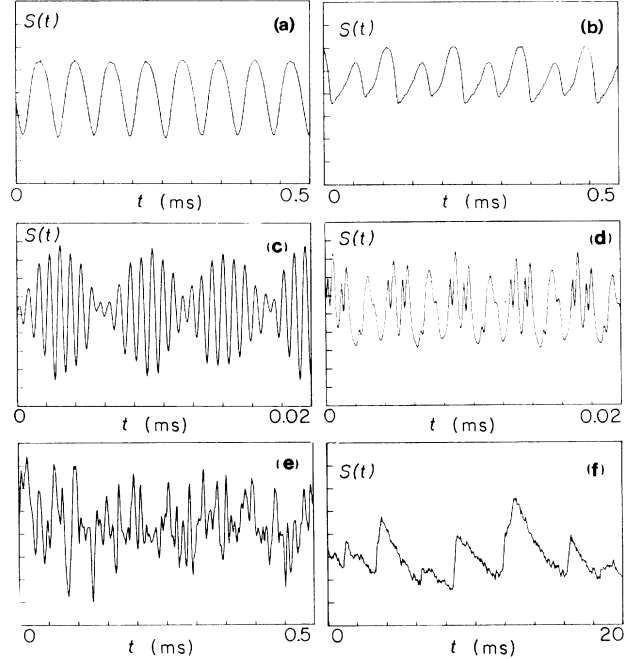


FIG. 3. Observed ac signals $S(t)$ in spin-wave instability showing (a) periodic oscillation at 16 kHz; (b) period doubled; (c) quasiperiodic; (d) frequency locking; (e) chaotic; (f) aperiodic relaxation oscillation.

tem then displays quasiperiodicity, including frequency locking [Fig. 3(d)] and chaos, also predicted by the model. In the dashed-line region labeled "very noisy collective oscillations" there is a fairly abrupt onset of a higher-level base line. In yet another region of Fig. 1, we find so-called "relaxation oscillations" and irregular narrow spikes with no spectral peaks.

We model the system as a collection of coupled quantum oscillators.¹⁸ The Hamiltonian includes the resonator mode (R), uniform mode (B), and spin waves b_k with energies ω_p , ω_0 , and ω_k , respectively. These oscillators are mutually coupled with coupling constants G between R and B , g_k between B and b_k , and four-magnon interactions $T_{kk'}$, $S_{kk'}$ among $\{b_k\}$. The driving field $P_{in}^{1/2} \times \exp(-i\omega_p t)$ couples with R . From the Hamiltonian, we obtain the equations of motion for R , B , and b_k , and add phenomenological damping terms with their constants Γ , γ_0 , and γ_k , respectively. We transform to slow variables C_k via $b_k = C_k \exp(-i\omega_p t/2)$ and adiabatically eliminate R, B , assuming $\Gamma \gg \gamma_k$. We assume $C_k = C_{-k}$ and arrive at a set of coupled equations for C_k as

$$\dot{C}_k = -(\gamma_k + i\Delta\Omega_k)C_k - iQg_k^* P_{in}^{1/2} C_k^* - i \sum_{k'} \{2T_{kk'} |C_{k'}|^2 C_k + (S_{kk'} + E g_k g_k^*) C_k^2 C_k^*\}, \quad (1)$$

where $\Delta\Omega_k \equiv \omega_k - \omega_p/2 = 2\pi\Delta f_k$ is the detuning parameter, and parameters Q and E are functions of G , ω_0 , ω_p , Γ , and γ_0 .

The fixed points of Eq. (1) may be determined exactly if only one mode is excited. The equation $\dot{C}_k = 0$ may be put in the form of a point on a unit circle, $M + N |C_k|^2 = (C_k^*)^2 / |C_k|^2$, where $M = i(\gamma_k + i\Delta\Omega_k) / QP_{in}^{1/2} g_k^*$, and $N = -(2T_{kk} + S_{kk} + E |g_k|^2) / QP_{in}^{1/2} g_k^*$. The Suhl threshold occurs at $|M| = 1$. For $P_{in} > P_t$ (P_t = threshold power)

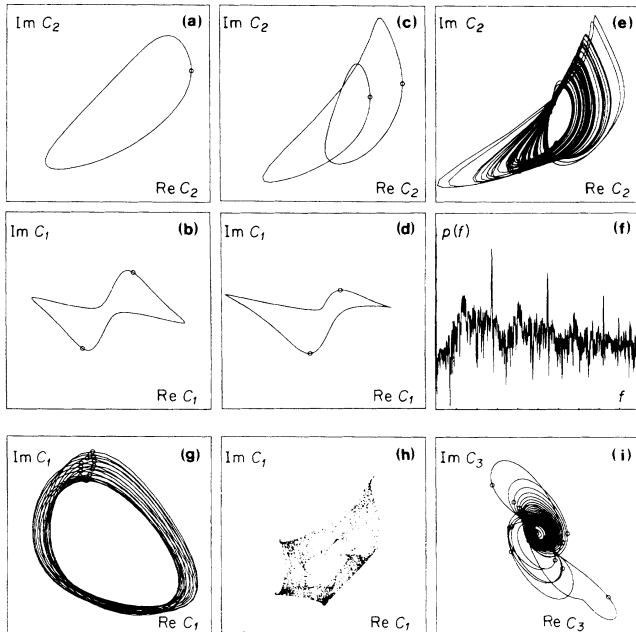


FIG. 4. (a) Computed behavior for two modes: phase portrait for periodic oscillations, asymmetric mode; $\Delta f_1 = -300$ kHz, $\Delta f_2 = 200$ kHz. (b) Symmetric mode. (c) Period doubling of asymmetric mode; $\Delta f_1 = -385$ kHz, $\Delta f_2 = 115$ kHz. (d) Symmetry breaking of symmetric mode. (e) Chaotic orbit following period doubling cascade; $\Delta f_1 = -410$ kHz, $\Delta f_2 = 90$ kHz. (f) Power spectrum of chaotic orbit, $f_{\max} = 2.5$ MHz. (g) Computed phase portrait for quasiperiodic behavior for three modes, with Poincaré section. (h) Poincaré section of chaotic orbit; proximity to period-5 locking produces the five points. (i) Chaotic bursts.

the stability of the trivial fixed point ($C_k = 0$) is lost in a symmetry-breaking bifurcation. This occurs in two forms: (1) If $\text{Re}(M/N) > 0$, one obtains a supercritical bifurcation in which stable nonzero fixed points emerge from the origin as P_{in} crosses P_t . (2) For $\text{Re}(M/N) < 0$ a subcritical bifurcation occurs in which stable nonzero fixed points appear below P_t , and the system will jump to these at $P_{\text{in}} = P_t$, resulting in hysteretic behavior. The experimentally observed hysteresis is probably a related effect involving the cooperation of neighboring modes.

To explore the behavior of Eq. (1) we perform a numerical iteration¹⁹ for $N=1$, then $N=2$, etc. For $N=1$, the system is always attracted to a fixed point, but a hysteresis may be displayed as noted above. For $N=2$, periodic oscillations are found [Figs. 4(a) and 4(b)]: Mode 2 exhibits an asymmetric orbit while mode 1 exhibits a symmetrical orbit at twice the period. We simulate the spatial modes of Fig. 2 by choosing $\Delta f_1 = f_s - 500$ kHz and $\Delta f_2 = f_s$, and shift f_s to simulate the dc field shift. The computed behavior [Figs. 4(c) and 4(d)] shows period doubling and symmetry breaking, respectively, and eventually chaotic behavior [Figs. 4(e) and

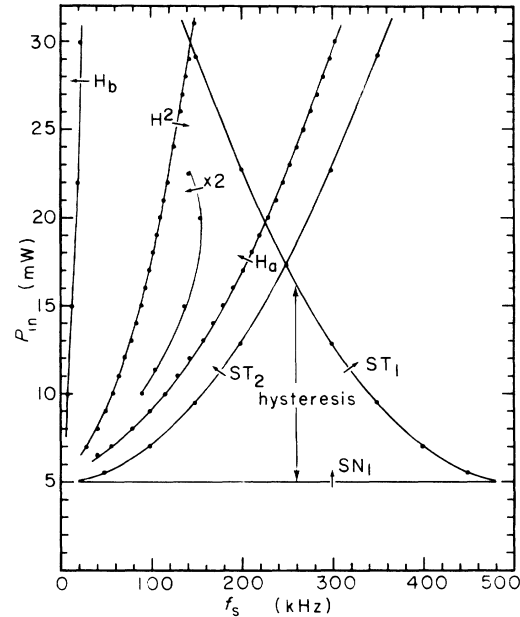


FIG. 5. Computed parameter-space diagram for the model, Eq. (1), for up to three active modes.

4(f)] for both modes.

For $N=3$ modes, new behavior arises: Figure 4(g) shows quasiperiodic behavior with a smooth Poincaré section of a torus; at higher excitation the section [Fig. 4(h)] is a chaotic attractor. For some other parameter values the behavior shows chaotic bursts [Fig. 4(i)] and other forms of aperiodic behavior similar to that observed [Fig. 3(f)]. The computed behavior in parameter space (P_{in}, f_s) is shown in Fig. 5 for active participation of one, two, or three modes ($\Delta f_3 = f_s + 500$ kHz). The boundaries ST and SN are the absorption thresholds for increasing and decreasing P_{in} , respectively, showing hysteresis; H_a is the boundary for a Hopf bifurcation to a limit cycle which shows period doubling at the $\times 2$ boundary; the line H^2 is a secondary Hopf bifurcation to quasiperiodicity involving modes 1, 2, and 3; in the upper central region we find more exotic behavior.

To summarize, these new experimental findings for the first-order perpendicular pumping exhibit rich structures comparable to those of chaos and turbulence in fluid dynamics. These results, together with numerical computations from the model, give a surprisingly good picture of spin-wave dynamics in the chaotic regime.

This work was supported in part by the U.S. Department of Energy under Contract No. DE-AC03-76SF00098, and by the U.S. Office of Naval Research under Contract No. N00014-86-K-0154.

(a)Present address: Institute for Pure and Applied Physical Sciences, University of California, San Diego, La Jolla, CA 92093.

- ¹R. W. Damon, *Rev. Mod. Phys.* **25**, 239 (1953).
²N. Bloembergen and S. Wang, *Phys. Rev.* **93**, 72 (1954).
³H. Suhl, *J. Phys. Chem. Solids* **1**, 209 (1957).
⁴K. Nakamura, S. Ohta, and K. Kawasaki, *J. Phys. C* **15**, L143 (1982), and *J. Phys. Soc. Jpn.* **52**, 147 (1983).
⁵G. Gibson and C. Jeffries, *Phys. Rev. A* **29**, 811 (1984).
⁶S. Ohta and K. Nakamura, *J. Phys. C* **16**, L605 (1983).
⁷X. Y. Zhang and H. Suhl, *Phys. Rev. A* **32**, 2530 (1985); H. Suhl and X. Y. Zhang, *Phys. Rev. Lett.* **57**, 1480 (1986).
⁸S. M. Rezende, O. F. de Alcontara Bonfin, and F. M. de Aguiar, *Phys. Rev. B* **33**, 5153 (1986).
⁹X. Y. Zhang and H. Suhl, to be published.
¹⁰F. Waldner, D. R. Barberis, and H. Yamazaki, *Phys. Rev. A* **31**, 420 (1985).
¹¹F. M. de Aguiar and S. M. Rezende, *Phys. Rev. Lett.* **56**, 1070 (1986).
¹²M. Mino and H. Yamazaki, *J. Phys. Soc. Jpn.* **55**, 4168 (1986); H. Yamazaki and M. Warden, *J. Phys. Soc. Jpn.* **55**, 4477 (1986).
¹³T. L. Carroll, L. M. Pecora, and F. J. Ratchford, *Phys. Rev. Lett.* **59**, 2891 (1987).
¹⁴P. H. Bryant, Ph.D. thesis, University of California, 1987 (unpublished).
¹⁵A. M. Clogston, H. Suhl, L. R. Walker, and P. W. Anderson, *J. Phys. Chem. Solids* **1**, 129 (1956).
¹⁶W. Jantz and J. Schneider, *Phys. Status Solidi (a)* **31**, 595 (1975).
¹⁷V. V. Zautkin, V. S. L'vov, and S. S. Starobinets, *Zh. Eksp. Teor. Fiz.* **63**, 182 (1973) [*Sov. Phys. JETP* **36**, 96 (1973)].
¹⁸P. H. Bryant, C. D. Jeffries, and K. Nakamura, to be published.
¹⁹Typical parameter values used: $P_{in} = 0.015$ W; $\gamma_k = 1 \times 10^6$ s⁻¹; $iQg_k = 1.414 \times 10^7$ W^{-1/2} s⁻¹; $S_{kk'} = S_{kk} = 4.3 \times 10^{-8}$ s⁻¹; $T_{kk'} = -2 \times 10^{-8}$ s⁻¹; $T_{kk} = 0$; $E = 0$.

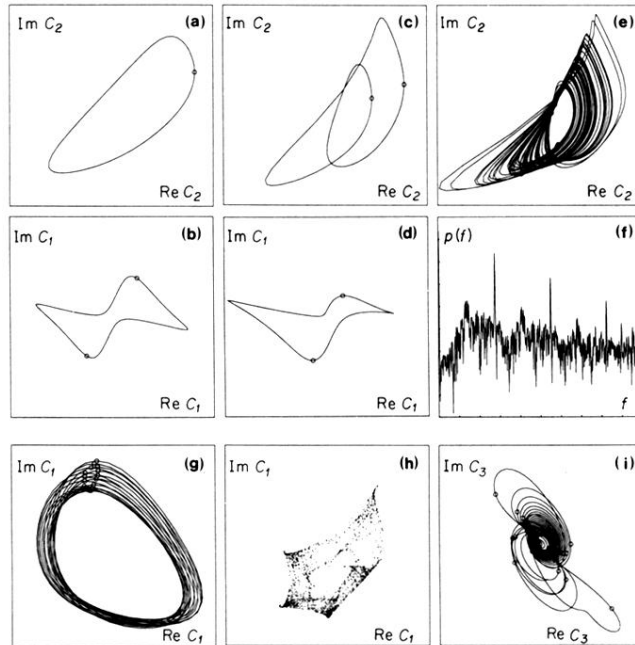


FIG. 4. (a) Computed behavior for two modes: phase portrait for periodic oscillations, asymmetric mode; $\Delta f_1 = -300$ kHz, $\Delta f_2 = 200$ kHz. (b) Symmetric mode. (c) Period doubling of asymmetric mode; $\Delta f_1 = -385$ kHz, $\Delta f_2 = 115$ kHz. (d) Symmetry breaking of symmetric mode. (e) Chaotic orbit following period doubling cascade; $\Delta f_1 = -410$ kHz, $\Delta f_2 = 90$ kHz. (f) Power spectrum of chaotic orbit, $f_{\max} = 2.5$ MHz. (g) Computed phase portrait for quasiperiodic behavior for three modes, with Poincaré section. (h) Poincaré section of chaotic orbit; proximity to period-5 locking produces the five points. (i) Chaotic bursts.